Transient Receptor Potential Vanilloid Type 1 Protects Against Pressure Overload–Induced Cardiac Hypertrophy by Promoting Mitochondria-Associated Endoplasmic Reticulum Membranes

Yuxiang Wang, MD,† Xiuchuan Li, PhD,† Xiaoli Xu, BS,‡ Xuemei Qu, PhD,‡
and Yongjian Yang, MD, PhD*†*

Abstract: Transient receptor potential vanilloid type 1 (TRPV1) is a nonselective cation channel that mediates the relationship between mitochondrial function and pathological myocardial hypertrophy. However, its underlying mechanisms remain unclear. This study aimed to investigate whether TRPV1 activation improves the morphology and function of intracellular mitochondria to protect cardiomyocytes after pressure overload-induced myocardial hypertrophy. The myocardial hypertrophy model was established by performing transverse aortic constriction surgery in C57BL/6 J male mice. The data revealed that TRPV1 activation significantly reduced myocardial hypertrophy, promoted ejection fraction% and fractional shortening%, and decreased the left ventricular internal diameter in end-diastole and left ventricular internal diameter in end-systole after transverse aortic constriction. Moreover, in vitro experiments revealed that TRPV1 reduces cardiomyocyte area and improves mitochondrial function by promoting mitochondria-associated endoplasmic reticulum membranes (MAMs) formation in a phenylephrine-treated cardiomyocyte hypertrophy model. TRPV1 up-regulates the phosphorylation levels of AMP-activated protein kinase and expression of mitofusin2 (MFN2). TRPV1 function is blocked by single-stranded RNA interfering with silent interfering MFN2. Activation of TRPV1 reduced mitochondrial reactive oxygen species caused by phenylephrine, whereas disruption of MAMs by siMFN2 abolished TRPV1-mediated mitochondrial protection. Our findings suggest that TRPV1 effectively protects against pressure overload-induced cardiac hypertrophy by promoting MAM formation and conserved mitochondrial function via the AMP-activated protein kinase/MFN2 pathway in cardiomyocytes.

Key Words: TRPV1, MAMs, myocardial hypertrophy, mitochondrial

INTRODUCTION

Uncontrolled hypertension and aortic stenosis increase afterload. In response to pressure overload, cardiomyocyte size increases, leading to adverse cardiac remodeling, myocardial dysfunction, capillary rarefaction, interstitial fibrosis, and heart failure.[1] Cardiac hypertrophy is an important prepathology of heart failure. However, the mechanisms underlying pathological cardiac hypertrophy remain largely unknown. At the cellular level, cardiomyocyte hypertrophy is driven by changes in ion channels and metabolic remodeling.[1–3]

Transient receptor potential vanilloid type 1 (TRPV1) is a widely reported nonselective cation channel that may mediate the relationship between mitochondrial function and pathological myocardial hypertrophy.[4] The correlation between TRPV1 and myocardial hypertrophy is widely known.[4,5] A previous study showed that capsaicin, a TRPV1 agonist, could protect against high-salt-intake-induced left ventricular hypertrophy by reducing oxidative stress and inhibiting hypertrophic signaling pathways,[6,7] whereas the genetic ablation of TRPV1 exacerbates pressure overload-induced cardiac hypertrophy.[5] Because the role of TRPV1 in the pathogenesis of myocardial hypertrophy and the underlying molecular mechanisms remain unclear, the protective effect of TRPV1 on mitochondrial function could play a beneficial role in cardiomyocyte hypertrophy.[6–8] Further studies should focus on the mechanisms by which TRPV1 regulates mitochondrial function.

The complex network encompassing microdomains linking mitochondria and the endoplasmic reticulum (ER), named mitochondria-associated endoplasmic reticulum membranes (MAMs), regulates mitochondrial calcium transfer, mitochondrial oxidative capacity, and metabolism.[9,10] Studies have reported that disorders of cardiomyocyte mitochondrial

function regulated by MAMs could lead to the development of heart injuries such as diabetic cardiomyopathy and heart failure.[11–13] Mitofusin2 (MFN2) is an essential mitochondrial fusion protein and an adaptor for chaining the ER and mitochondria, playing an important role in MAM formation.[14,15]

Numerous studies have shown that MAM participates in mediating the initiation site of autophagosome formation and mitochondrial division.[16,17] Studies have reported that MFN2 is involved in the autophagy of cardiomyocytes, in which autophagosomes accumulate in MFN2 knockout cardiomyocytes because of impaired fusion of autophagosomes with lysosomes in the absence of MFN2.[18] This further proves that MFN2 promotes membrane integration. Some studies provided evidence that imbalanced mitochondrial dynamics induced by downregulated MFN2 contribute to the development of heart failure and diabetic cardiomyopathy.[19,20] MFN2 in diabetic hearts inhibits mitochondrial fission and prevents the progression of diabetic cardiomyopathy.[20]

AMP-activated protein kinase (AMPK), as a guardian for mitochondrial energy homeostasis, is responsible for mitochondrial fission, whereas MAM is involved in these processes.[21–23] AMPK dysfunction is ascribed to many cellular pathophysiological processes, such as diabetes, cancer, obesity, and cardiovascular disease.[24–27] Recent research has shown that, under energy stress, the AMPK-MFN2 axis regulates MAM dynamics, in which AMPK interacts with and phosphorylates MFN2, directly promoting MAM formation.[28] However, it is largely unknown how TRPV1 regulates MAM in myocardial hypertrophy.

In the present study, we detected the role of TRPV1 in cardiac hypertrophy and found that TRPV1 expression was increased in the myocardium of transverse aortic constriction (TAC) mice or phenylephrine (PE)-treated cardiomyocytes. Further studies used capsaicin to increase TRPV1 activity and reported that its activation improved mitochondrial function by increasing MAM formation. We explored whether TRPV1 activation promotes MAM formation through AMPK-MFN2 signaling in response to myocardial hypertrophy.

METHODS

TAC Mouse Model

Male C57BL/6 J mice (6-week-old) were purchased from SPF Biotechnology (Beijing, China). TAC surgery was performed as previously described.[29] Briefly, male mice were anesthetized with 2% isoflurane (Baxter, Guayama) and kept on a 37°C heated plate. Next, the thoracic cavity was opened. A curved needle was placed under the arch and perforated between the vascular wall and the connective tissue. The 6-0 monofilaments were sutured with a curved needle and pulled under the aortic arch. Next 27-gauge blunted needles were placed into the ring, the suture was secured with a double knot, and the blunt needle was gently removed. Finally, the contraction was confirmed with the knot position, and both ends of the suture were cut. An identical procedure was used for the sham surgery without suture placement. Three days after TAC surgery, mice were given normal standard chow (control group) or normal chow plus 0.01% capsaicin (capsaicin group; 0.01 g capsaicin per

100 g chow).[6] Eight weeks after surgery, the weights of the hearts were measured and photographed. Some hearts were fixed in 4% paraformaldehyde for histological analysis, whereas others were stored at −80°C for the biochemical analyses.

All animal manipulations were performed in strict accordance with the Guide for the Care and Use of Laboratory Animals of the National Institutes of Health (NIH) (Bethesda, MD). Formal approval to conduct the animal experiments described here was obtained from the Ethics Committee and the Institutional Animal Care and Use Committee of the General Hospital of Western Theater Command (2020ky012). All surgeries were performed with the animals under anesthesia. All efforts were made to minimize suffering and use only the number of animals necessary to produce reliable scientific data. No alternatives to animal experimentation are available for this type of experiment.

Echocardiography

Echocardiography was performed 8 weeks after the TAC or sham surgery. Cardiac function was assessed using a Vivid 9 high-frequency color Doppler ultrasound system and a 40-MHz transducer (GE Healthcare, Boston, MA) operated by a blinded and skilled technologist. The mice were anesthetized using 2% isoflurane (Baxter) and the heart rates were kept at 450–550 beats/min. Left ventricular internal dimensions at end-diastole and left ventricular internal dimensions at end-systole were measured under M-mode and B-mode from the left ventricular parasternal long axis. Fractional shortening (%) and ejection fraction (%) were calculated.

Neonatal Rat Cardiomyocytes Isolation, Culture, and Treatment

Neonatal rat cardiomyocytes were obtained as described previously.[30] One-day-old neonatal rats were rinsed quickly in 75% ethanol solution for surface sterilization. The pups were decapitated using sterile scissors (straight), and the chest was opened along the sternum to allow access to the chest cavity and heart. The hearts were isolated from the chest cavity, washed, and minced in phosphate buffered saline. The minced neonatal hearts were dispersed by enzymatic digestion with 1.25 mg/mL trypsin (Invitrogen, Carlsbad, CA) and 0.8 mg/mL collagenase II (Worthington, Lakewood, NJ).

After fibroblast removal by differential attachment for 90 minutes, the cardiomyocytes were plated in plates or slides according to the experimental requirements. DMEM/F12 medium (Gibco, Grand Island, NY) contained 10% fetal bovine serum (Gibco), 100 U/mL penicillin/streptomycin (Invitrogen), and 0.1 mmol/L bromodeoxyuridine (Beyotime, Jiangsu, China). Twenty-four hours after seeding, the cardiomyocytes were starved in serum-free medium and then treated with PE before the addition of drugs and exposed to 20 μM PE for 48 hours to induce hypertrophy. The drug sources and doses were as follows: Capsaicin (Cap; 1 μM), compound C (CC; 1 μM), PE (20 μM); all were purchased from MedChemExpress (Shanghai, China).

siRNA Transfections

Neonatal rat cardiomyocytes were transfected with MFN2 siRNA (50 nM; RiboBio, Guangdong, China) in

TABLE 1. List of siRNA

Target	Species	Sequence
Mfn2	Rat	CCTCTCCTTTGGACTGTAT

OPTI-MEM reduced serum media (Gibco) using lipofectamine RNAiMax transfection reagent (Invitrogen). All the siRNA sequences are listed in Table 1.

Heart Histology

Hearts from all groups were fixed with 4% paraformaldehyde. Dehydration and embedding in paraffin were performed using routine histological procedures. Subsequently, the samples were sectioned transversely at 4-μm thicknesses. The sections were stained with hematoxylin and eosin (Solarbio, Beijing, China) to determine the morphology of the whole heart and observed under a microscope (M8, Precise, Germany). For wheat germ agglutinin staining, the heart was cut in half by forming a transverse slice between the atrioventricular sulcus and apex. The base specimen was fixed in 10% formalin buffer, embedded in paraffin, and cut into 4-μm-thick sections.

The cross-sectional areas of the cardiomyocytes were measured in images captured in sections stained with 5 μM wheat germ agglutinin (Invitrogen) for 20 minutes at room temperature. The images were observed using a fluorescence microscope (Eclipse Ti-U; Nikon Corporation, Tokyo, Japan). The cross-sectional areas were measured in the papillary muscle zone, and a total of 5 sections per animal were analyzed to check for hypertrophy using ImageJ software (NIH, Bethesda, MD).

Transmission Electron Microscopy

Cells grown in 10-cm plastic dishes were fixed with 2% (w/v) glutaraldehyde buffered with 0.1 M sodium cacodylate at pH 7.4, for 2 hours at room temperature. The fixed cells were carefully detached using a plastic cell scraper, collected into Eppendorf tubes, and centrifuged to obtain a pellet. The samples were further incubated with 2% osmium tetroxide and 0.1 mM sodium cacodylate (pH 7.4) for 1 hour at 4°C. Ultrathin sections were stained with uranyl acetate and lead citrate and examined under a JEM-1400Plus electron microscope (Hitachi, Tokyo, Japan). ER-mitochondrial contacts were quantified as previously described.[31]

The images were analyzed using ImageJ software (NIH). The mitochondrial and ER membranes were delineated using the freehand tool of ImageJ (NIH). The selected areas were converted to masks (analysis module of ImageJ software), where the segmentation region of the ER and mitochondria were separated from the original image. The perimeters and distances of the ER and mitochondria (30 nm) were calculated. For MAM quantification, we normalized the length of total ER connected to the mitochondria to the total ER perimeter.

Endoplasmic Reticulum and Mitochondria Contact Analysis

The cells were labeled with MitoTracker Red (Beyotime) and ER-Tracker Green (Beyotime) and observed using a confocal microscope (Olympus AX70, Tokyo, Japan).

Pearson correlation analysis was used to quantify the degree of colocalization between the fluorophore ER and mitochondria.[32] Pearson's correlation coefficient was analyzed using the colocalization analysis module from ImageJ software (NIH).

Quantitative Real-Time Polymerase Chain Reaction

Total RNA was extracted from tissues or cells using TRIzol reagent (TaKaRa, Tokyo, Japan). Chloroform (0.2 mL) was added to each 1 mL of TRIzol, shaken vigorously for 15 seconds, and left at room temperature for 3 minutes. Centrifugation at 10,000*g* at 4°C for 15 minutes. The sample consisted of 3 layers: a yellow organic phase (bottom); a colorless aqueous phase (upper); and an intermediate layer. RNA was mainly present in the aqueous phase. We transferred the water phase to a new tube; RNA in the aqueous phase was precipitated with isopropyl alcohol. We then added 0.5 mL of isopropyl alcohol to each 1 mL of TRIzol and allowed it to stand at room temperature for 10 minutes.

After centrifugation at 4°C for 10 minutes at 10,000*g*, no RNA precipitation was observed before centrifugation, whereas a gelatinous precipitation appeared at the side and bottom of the tube after centrifugation. We then removed the supernatant. The RNA precipitate was washed with 75% ethanol. At least 1 mL of 75% ethanol was added to every 1 mL of TRIzol. The mixture was centrifuged for 5 minutes at 7500*g* at 4°C, and the supernatant was discarded. The RNA precipitates were dried at room temperature for approximately 5–10 minutes.

One microgram of RNA was used to synthesize cDNA using PrimeScript RT Master Mix (TaKaRa) following the

TABLE 2. List of PCR Primers

Target	Species	Application
ANP	Rat	Fwd: 5′- TGAGCCGAGACAGCAAACAT -3′
		Rev: 5′- CAATATGGCCTGGGAGCCAA -3′
BNP	Rat	Fwd: 5′- CAGAAGCTGCTGGAGCTGATA -3′
		Rev: 5′- GGCGCTGTCTTGAGACCTAA -3′
β-MHC	Rat	Fwd: 5′- CCGAGTCCCAGGTCAACAAG -3′
		Rev: 5′- CTTGGAGCTGGGTAGCACAA -3′
TRPV1	Rat	Fwd: 5′- TTGGTGGAGAATGGAGCAG -3′
TRPV1	Mouse	Rev: 5′- TGTGTTATCTGCCACCTCCA -3′
		Rev: 5′- ATTGCTCTGCTCCTGGACAT -3′
		Fwd: 5′- TTCTCCACCAAGAGGGTCAC -3′
Mfn2	Rat	Fwd: 5′- TCCATCGTCACCGTCAAGAAG -3′
		Rev: 5′- TGGCAGTGACAAAGTGCTTGAG -3′
GAPDH	Rat	Fwd: 5′- GCCCAGCAAGGATACTGAGA -3′
		Rev: 5′- GATGGTATTCGAGAGAAGGGAGG -3′

manufacturer's instructions. Quantitative real-time PCR was performed using SYBR Green dye (TaKaRa). The primers used are shown in Table 2.

Western Blotting

Proteins were extracted from heart tissues or primary cardiomyocytes with ice-cold tissue extraction reagent (Beyotime) containing a protease inhibitor cocktail (Roche, Indianapolis, IN) and phosphatase inhibitor cocktail (Sigma-Aldrich, St. Louis, MO). The homogenate was sonicated and kept on ice for 1 hour. The lysate was centrifuged at $12,000g$ for 30 minutes. The supernatants were boiled in loading buffer (Solarbio) for 10 minutes at $100°C$, and the samples were stored at $-20°C$ before use. Protein samples (30 μg) were separated by sodium dodecyl sulfate–polyacrylamide gel electrophoresis on a 10% or 15% polyacrylamide gel and electrotransferred to nitrocellulose membranes.

After the nonspecific binding sites were blocked in Tris-buffered saline containing 5% nonfat dry milk for 1 hour, the membranes were incubated at $4°C$ overnight with primary antibodies, including mouse anti-TRPV1 (1:1000; cat. No. sc-398417; Santa Cruz Biotechnology, Santa Cruz, CA), rabbit anti–voltage-dependent anion channels (1:1000; cat. No. 10866-1-AP; Proteintech, Wuhan, China), rabbit anti-inositol 1,4,5-trisphosphate receptor (IP3R) (1:1000; cat. No. 19962-1-AP; Proteintech), rabbit anti-P-AMPK (1:1000; cat. No. 8208; Cell Signaling Technology, Danvers, MA), rabbit anti-AMPK (1:1000; cat. No. 5832; Cell Signaling Technology), rabbit anti-MFN2 (1:1000; cat. No. 12186-1-AP; Proteintech), rabbit anti-atrial natriuretic peptide (ANP) (1:500; cat. No. 27426-1-AP; Proteintech), rabbit anti-B-type natriuretic peptide (BNP) (1:500; cat. No. 13299-1-AP; Proteintech), and rabbit anti-beta-myosin heavy chain (β-MHC) (1:500; cat. No. 10799-1-AP; Proteintech). Mouse anti-GAPDH antibody (1:5000; cat. No. 60004-1-lg; Proteintech) was used as an internal control. The membranes were then washed and incubated with IRDye680-labeled goat anti-rabbit (1:10,000; cat. No. 926–68071; Li-Cor Biosciences, Lincoln, NE) or IRDye800-labeled goat anti-mouse secondary antibody (1:10,000; cat. No. 926–68070; Li-Cor Biosciences) at room temperature for 1 hour. The membranes were washed 3 times in Tris-buffered saline with Tween-20, and the bands were detected using an Odyssey Infrared Imaging System (Li-Cor Biosciences). The images were analyzed using the Odyssey Application Software to obtain integrated intensities. ImageJ software (NIH) was used to analyze the average gray value of each band.
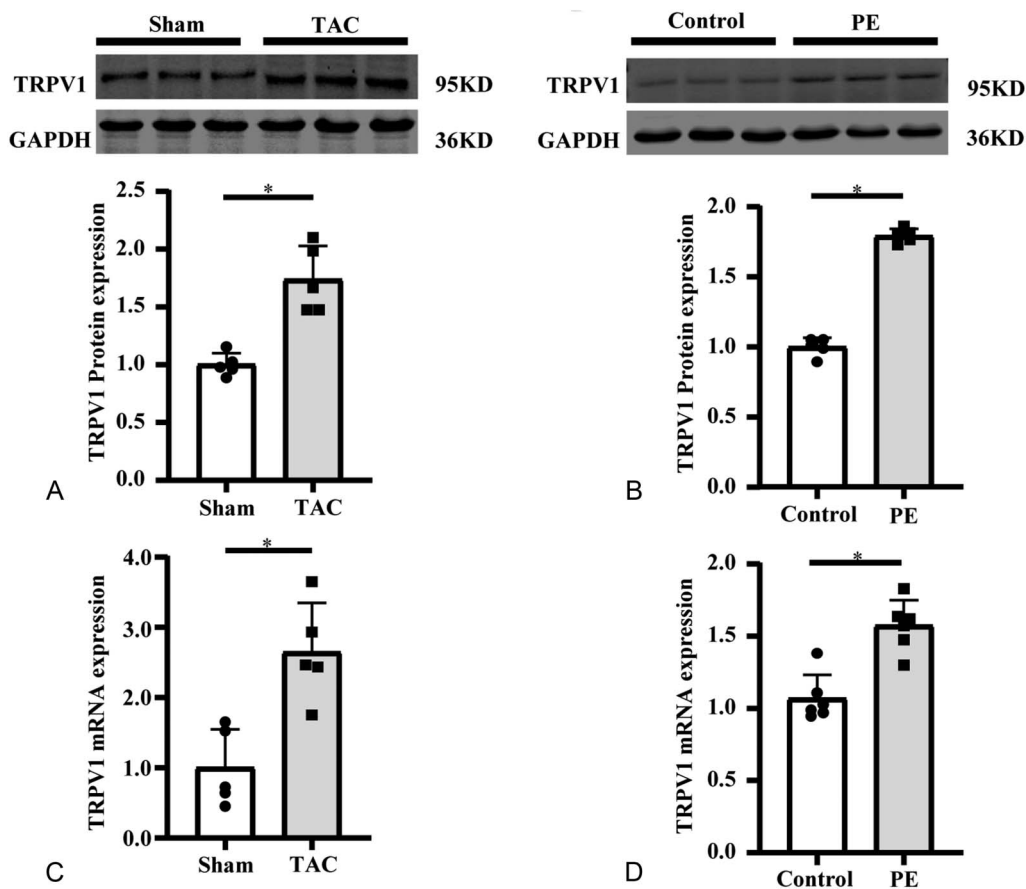

FIGURE 1. Pressure overload increased TRPV1 expression in myocardium and cardiomyocytes. TRPV1 protein and mRNA expression in myocardium following TAC (A and C). PE-treated neonatal rat cardiomyocytes (B and D) were detected by immunoblotting and reverse transcription polymerase chain reaction. n = 6 per group. *$P < 0.05$ compared with sham or control.
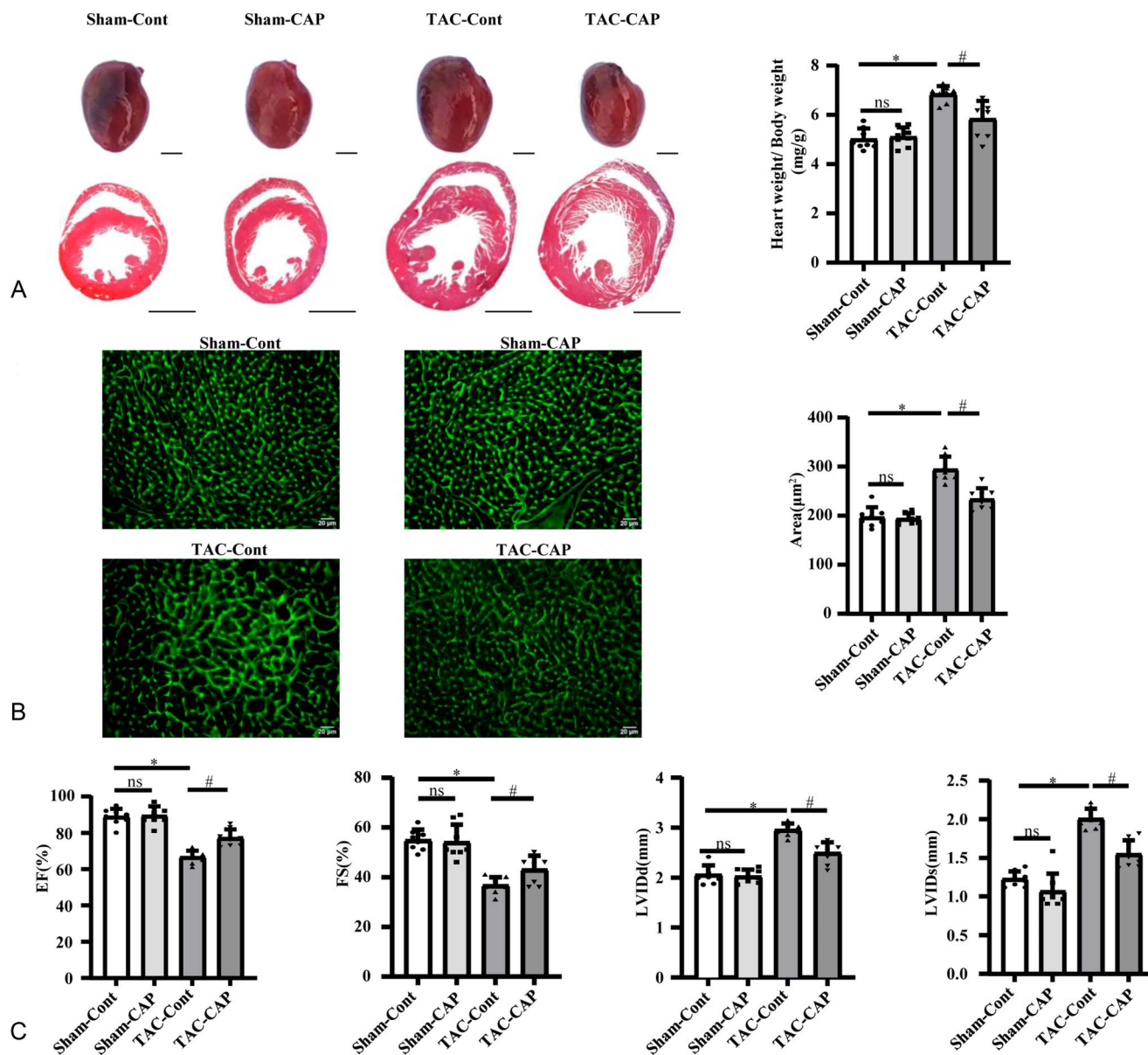
FIGURE 2. TRPV1 activation alleviated pressure overload–induced myocardial hypertrophy. A, Histological analysis of heart sections from normal diet (Cont)-fed or capsaicin diet (CAP)-fed mice with or without TAC (scale bar = 1 mm). Heart weight to body weight ratio in the indicated groups. B, Heart cross-sections were stained with wheat germ agglutinin and the average cross-sectional areas of cardiomyocytes were quantified (scale bar = 20 μm). C, The echocardiographic assessment of cardiac function from normal diet-fed or CAP-fed mice. The animal experiments were performed 8 weeks after TAC surgery, n = 8 mice per group. *$P < 0.05$ compared with sham-cont, #$P < 0.05$ compared with TAC-cont group.

Immunoprecipitation

Equal amounts of cell lysates (1000 μg total protein) were incubated with an anti-IP3R antibody (4 μg; cat. No. 19962-1-AP; Proteintech) overnight at 4°C. Next, 50 μL of protein G Plus-agarose beads (Santa Cruz Biotechnology) were added, and the lysates were incubated for another 4 hours at 4°C. The beads were washed 3 times in lysis buffer, and the proteins were eluted with loading buffer by boiling at 100°C for 15 minutes. The elution was then analyzed by western blotting for voltage-dependent anion channels (1:1000; cat. No. 10866-1-AP; Proteintech).

Immunofluorescence

Primary cardiomyocytes were fixed with 4% paraformaldehyde (v/v) in EZ slides (Millipore, Billerica, MA) for 15 minutes, permeabilized with 0.3% Triton X-100 (v/v) for 15 minutes, and blocked with 5% bovine serum albumin for 30 minutes at room temperature. The cells were incubated with mouse anticardiac troponin T (cTnT) primary antibodies (1:100; cat. No. MA5-12960; Invitrogen) overnight at 4°C, followed by Alexa Fluor 488-conjugated secondary antibodies (1:100; cat. No. A32723; Invitrogen)
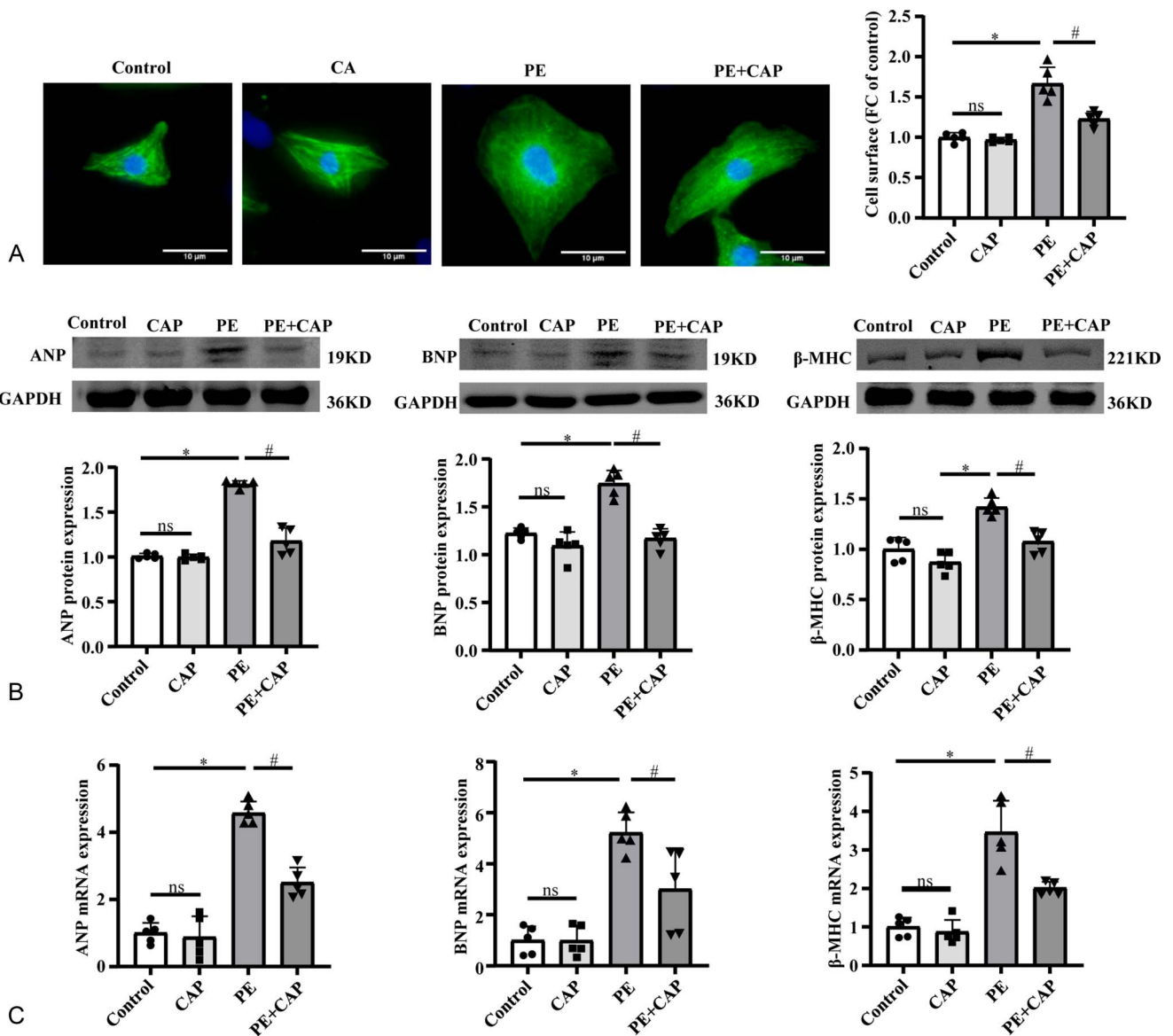
FIGURE 3. TRPV1 activation protected against PE-induced cardiomyocyte hypertrophy in vitro. A, Representative images and analysis of the cell surface area of neonatal rat cardiomyocytes stained with cTnT (green) and DAPI (blue) (n = 5, scale bar = 10 μm). B, The ANP, BNP, β-MHC protein expression in primary cardiomyocytes treated with capsaicin and PE (n = 5). C, Quantitative polymerase chain reaction analyses of the mRNA levels of ANP, BNP, β-MHC in the indicated groups. n = 5 per group. *$P < 0.05$ compared with control, #$P < 0.05$ compared with PE group.

at 37°C for 45 minutes. Finally, the cells were stained with DAPI (Solarbio) at room temperature for 5 minutes. Images were captured using an Olympus AX70 laser confocal microscope at excitation wavelengths of 495 nm or 358 nm and detected at 518 nm or 461 nm.

Measurement of Mitochondrial Membrane Potential

A mitochondrial membrane potential (MMP) assay kit with JC-1 (Beyotime) was used to evaluate the MMP, whereas the fluorescence intensity of the JC-1 monomers/aggregates (green fluorescence for monomer, red fluorescence for aggregate) was measured by fluorescence microscopy (Eclipse Ti-U, Nikon Corporation) following the manufacturer's instructions. Digital images were analyzed using ImageJ software (NIH). The calculation results of the red/green fluorescence ratio were used to assess MMP.

Mitochondria ROS Measurements

Mitochondrial reactive oxygen species (ROS) activity was detected using the fluorescent probe MitoSOX (Invitrogen).[33] Briefly, cardiomyocytes were incubated with 5 μM MitoSOX (red fluorescence) in PBS and DAPI (Beyotime Biotechnology, China) at 37°C in the dark for 10 minutes. The fluorescence

intensity of mitochondria ROS probes was measured by fluorescence microscopy (Eclipse Ti-U, Nikon Corporation). Digital images were analyzed using ImageJ software (NIH). The calculation results of the red fluorescence were used to assess mitochondrial ROS.

Measurement of ATP Levels

ATP content was detected using an ATP assay kit (Beyotime) according to the manufacturer's instructions. Briefly, cardiomyocytes were lysed with ATP assay buffer and mixed with fluorometric reaction mixture by gentle shaking. The sample fluorescence was measured using Varioskan Flash (Thermo Scientific, MA).

Statistical Analysis

The data involved in this article were subject to normal distribution through Shapiro–Wilk test. Data are shown as means ± SEM. Student's t-tests were performed to evaluate the statistical significance between 2 groups, and one-way analysis of variance was used to evaluate the statistical significance of more than 2 groups, and Tukey's post-hoc test was used for pair-wise comparison between the means when analysis of variance test was significant. All statistical analyses were performed using GraphPad Prism 8 (GraphPad Software, San Diego, CA). Statistical significance was set at $P < 0.05$.

RESULTS

Pressure Overload Increased TRPV1 Expression in Myocardium and Cardiomyocytes

The TAC mouse model was used to check the changes in TRPV1 expression in the myocardium and cardiomyocytes.

We found that TAC increased the protein and mRNA expressions of TRPV1 in hypertrophic heart tissues (Figs. 1A, C). Similar observations were made with cardiomyocytes subjected to PE treatment (Figs. 1B, D).

Activated TRPV1 Alleviated Pressure Overload–Induced Myocardial Hypertrophy

To further elucidate the physiological role of TRPV1 in myocardial hypertrophy, the TRPV1 agonist capsaicin was used to activate TRPV1 in TAC mice. Our data showed that TAC increased the heart weight to body weight ratio and cardiomyocyte area, while capsaicin significantly reduced the myocardial hypertrophy (Figs. 2A, B). Heart ultrasound analysis showed that the hallmarks of heart function were impaired, whereas capsaicin promoted the ejection fraction % and fractional shortening% and decreased the left ventricular internal diameter in end-diastole and left ventricular internal diameter in end-systole (Fig. 2C). Moreover, PE treatment induced cardiomyocyte hypertrophy, as shown by cTnT staining (Fig. 3A), and increased the protein and mRNA expression of hypertrophic signals such as ANP, BNP, and β-MHC (Figs. 3B, C). Capsaicin treatment partially restored cardiomyocyte area and ANP, BNP, and β-MHC protein and mRNA expressions (Figs. 3B, C). These results demonstrate that TRPV1 plays a protective role in the pathogenesis of myocardial hypertrophy.

TRPV1 Activation Protects Mitochondria by Promoting MAMs During Myocardial Hypertrophy

Since TRPV1 regulates mitochondria,[34] electron microscopy analysis showed that PE led to marked swelling and disruption of mitochondrial cristae in cardiomyocytes.

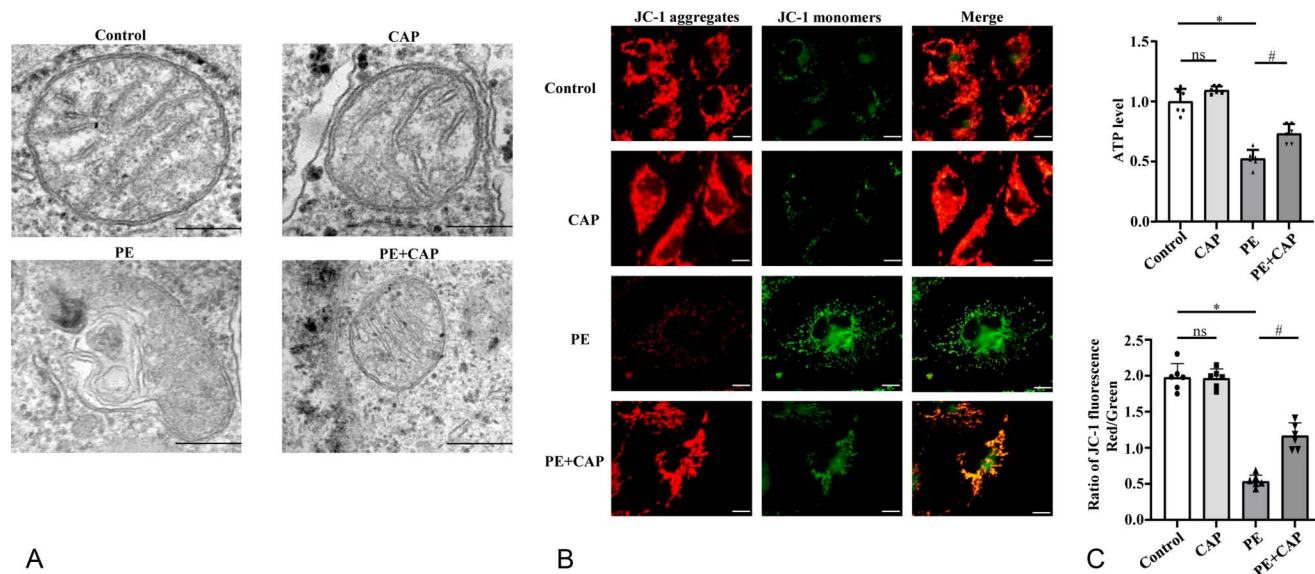**FIGURE 4.** TRPV1 activation attenuated mitochondrial dysfunction in cardiomyocytes. A, The mitochondrial morphology was observed by transmission electron microscopy (scale bar = 200 nm). B, MMP was assessed using a JC-1 kit. The JC-1 aggregate/JC-1 monomer ratio was measured for MMP. (n = 6, scale bar = 10 μm). C, ATP levels in cultured cardiomyocytes (n = 6). *$P < 0.05$ compared with control, #$P < 0.05$ compared with PE group.
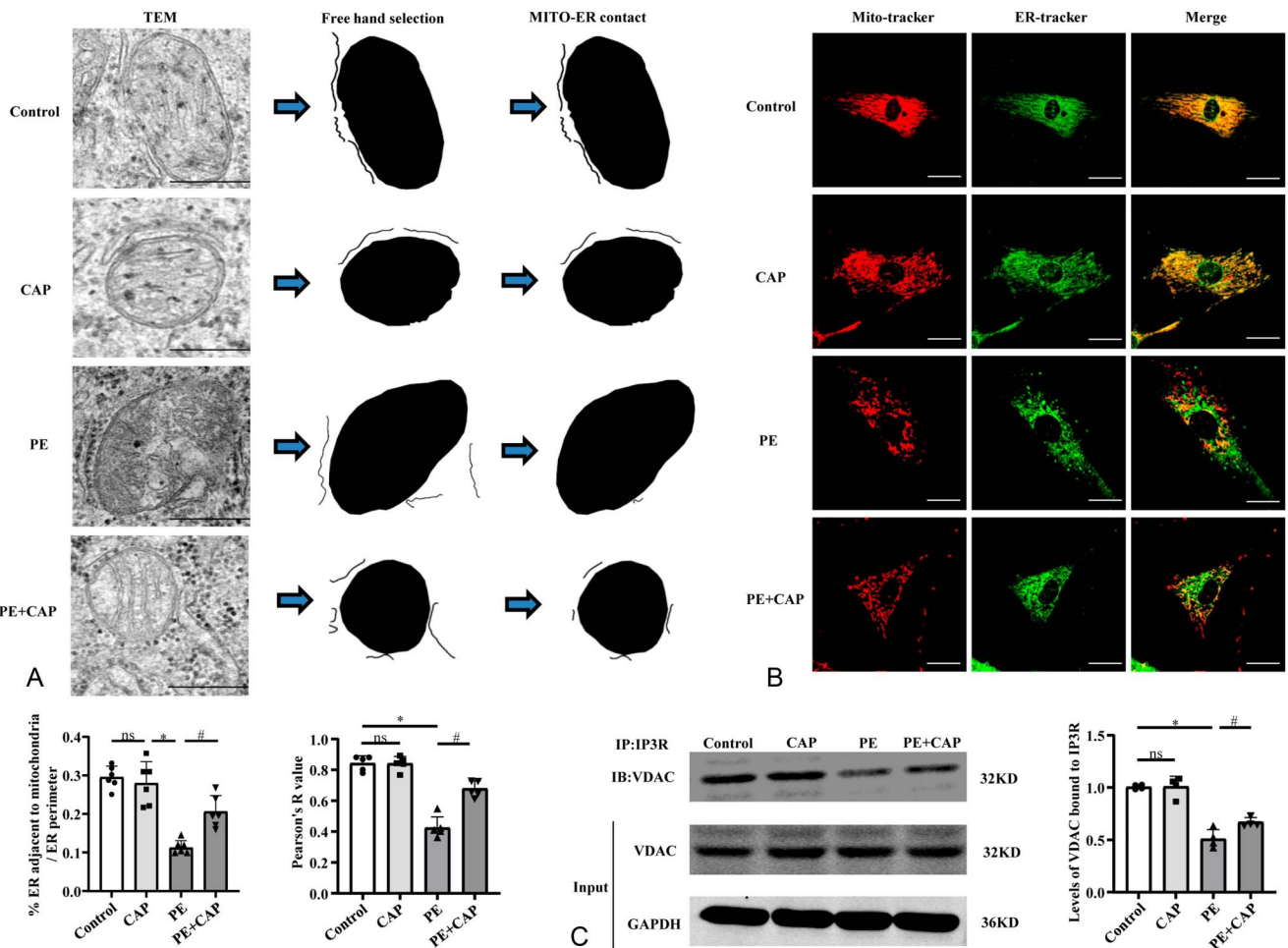
FIGURE 5. TRPV1 activation promoted MAM formation in cardiomyocytes. A, Representative transmission electron microscopy image indicating the ER and mitochondrial contacts in cardiomyocytes. Mitochondria and ER were delimitated using the free hand selection tool of ImageJ (NIH). Masks were generated with corresponding object identification (scale bar = 200 nm). Quantification of the ER adjacent to the mitochondria in cardiomyocytes was normalized by total ER length (n = 6). B, Representative confocal images showing the association between ER (ER-Tracker Green) and mitochondria (MitoTracker Red) in cardiomyocytes (scale bar = 10 μm). Quantitation of ER-mitochondria contacts using Pearson's coefficient (n = 5). C, The interaction between voltage-dependent anion channels and IP3R in cardiomyocytes was determined by IP and WB (n = 4). The bar chart shows levels of voltage-dependent anion channels bound to IP3R in the immunoprecipitations following quantification of signals from immunoblots. Voltage-dependent anion channels signals were normalized to GAPDH signals. *$P < 0.05$ compared with control, #$P < 0.05$ compared with PE group.

Capsaicin treatment alleviated PE-induced mitochondrial injury (Fig. 4A). The MMP and ATP production levels were decreased in PE-injured cells, and capsaicin increased MMP and ATP production in cardiomyocytes subjected to PE treatment (Figs. 4B, C).

To understand the potential role of MAMs in TRPV1-mediated protection of mitochondrial function, we used electron microscopy to examine MAM formation, which was determined as thin sheets aligned with mitochondria, with the distance between the 2 organelles less than 30 nm.[10,13] We found that the percentage of MAMs per ER was decreased in cardiomyocytes following PE treatment, while TRPV1 activation promoted MAM formation (Fig. 5A). Moreover, we observed a low degree of colocalization between mitochondria and ER. The colocalization of

mitochondria and ER increased when capsaicin was used (Fig. 5B). Next, we performed co-immunoprecipitation and found that cardiomyocytes subjected to PE with TRPV1 activation displayed higher physical interaction between IP3R, a protein marker of ER, and VADC, a protein marker of mitochondria, compared with PE-treated cells without capsaicin (Fig. 5C).

TRPV1 Activation Promotes MAM Formation Via AMPK/MFN2 Pathway

Because AMPK/MFN2 reportedly facilitates MAM formation,[28] we determined whether AMPK/MFN2 was involved in the protective effect of TRPV1 on mitochondria. As described previously, capsaicin rescued MMP and ATP production in PE-treated cardiomyocytes. Furthermore,

capsaicin reduced mitochondrial ROS, whereas disruption of MAM by siMFN2 abolished capsaicin-mediated mitochondrial protection and enhanced cell sizes (Figs. 6A–D).

Meanwhile, AMPK phosphorylation and MFN2 expression were decreased in PE-treated cardiomyocytes, and capsaicin partially restored the AMPK phosphorylation level and MFN2 intensity; however, the restorative effect was destroyed by the addition of the AMPK inhibitor CC (Fig. 7A). Likewise, although capsaicin-mediated mitochondrial recovery effect on PE generated a reduced colocalization between mitochondria and ER, the AMPK inhibitor CC could counteract this effect (Fig. 7B). These findings indicate that TRPV1 activation promotes MAM formation through the AMPK/MFN2 pathway.

DISCUSSION

The data presented here are consistent with the hypothesis that TRPV1 activation alleviates pressure overload-induced myocardial hypertrophy by improving mitochondrial function, which is ascribed to the promotion of MAM formation. As expected, the AMPK/MFN2 pathway is involved in TRPV1-mediated MAM formation.

As a receptor and ion channel, TRPV1 has a variety of physiological and pathological functions, such as pain, immunity, inflammation, and respiratory and cardiovascular diseases[35–38] and a protective effect on liver, kidney, and myocardial ischemia-reperfusion injury,[39–41] in which TRPV1 reduces the infarct area.

AMPK, as an energy sensor activated by TRPV1, exerts various regulatory mechanisms during the occurrence and development of diseases, including oxidative stress, autophagy, apoptosis, and mitochondrial functions.[21,42–44] Studies have shown that AMPK activation reduces mitochondrial damage, inhibits oxidative stress and apoptosis, and alleviates ischemia-reperfusion injury.[45]

MAM is a dynamic domain between the mitochondria and ER and structurally and functionally regulated by protein chains formed at specific subdomains of the ER.[46] Given the importance of MAM in regulating mitochondrial function, most diseases caused by abnormal MAM formation are associated with mitochondrial dysfunction, especially diabetic cardiomyopathy, ischemic cardiomyopathy, heart failure, and other heart diseases.[12,47] Here, we observed fluorescence staining of the mitochondria and ER during myocardial hypertrophy. The data show that the colocalization of the 2 organelles was significantly decreased and their interaction was impaired, indicating that MAM formation disorder plays an important role in myocardial hypertrophy. More importantly, we found that TRPV1 can increase the phosphorylation of AMPK, produce ATP, and promote MAM formation. These findings suggest that TRPV1-AMPK-MAM may be an underlying signaling pathway in the mediation of mitochondrial function and cardiac remodeling.

At the molecular level, mitochondrial dynamics are regulated by crucial mitochondrial membrane proteins. MFN2 in particular is a well-accepted fusion factor that
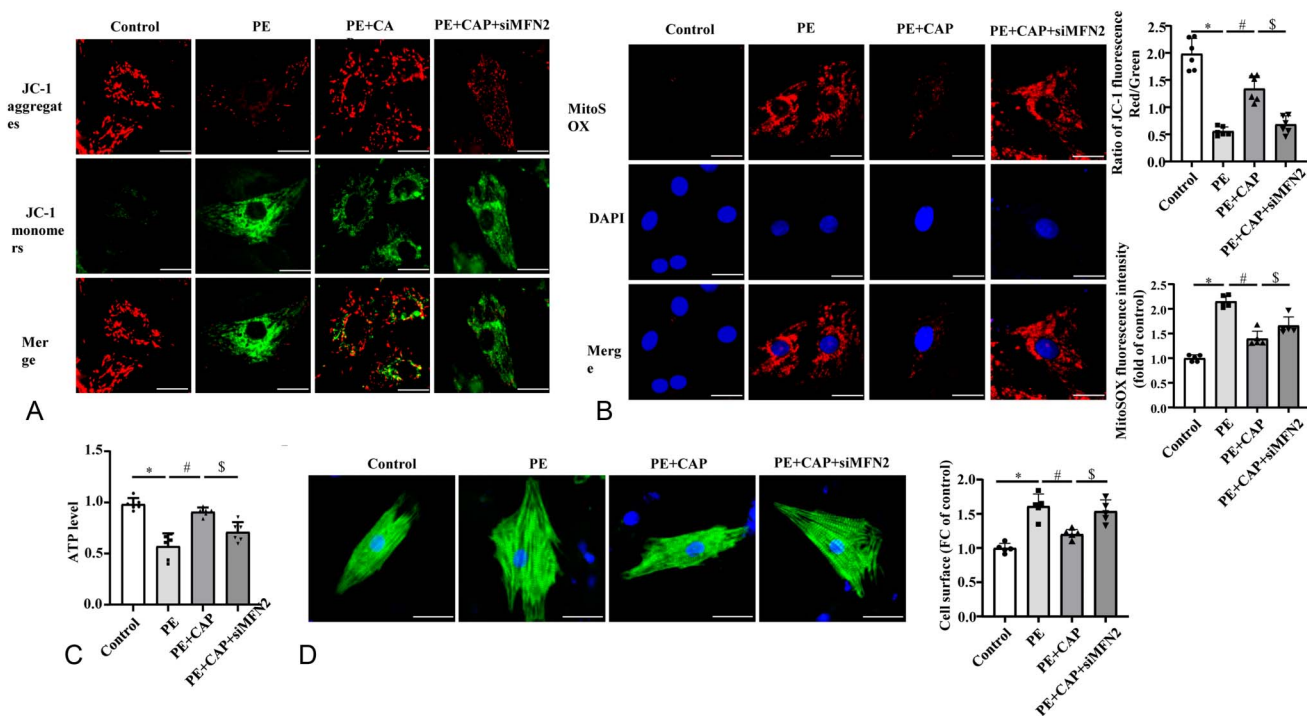

FIGURE 6. Disruption of MAM by siMFN2 abolished capsaicin-mediated mitochondria protection. A, MMP was assessed using a JC-1 kit. The JC-1 aggregate/JC-1 monomer ratio was measured for MMP (n = 6, scale bar = 10 μm). B, Effects of capsaicin on ROS production in PE-treated cardiomyocytes using MitoSOX red staining (n = 5, scale bar = 10 μm). C, ATP levels in cultured cardiomyocytes (n = 6). D, Representative images and analysis of the cell surface area of neonatal rat cardiomyocytes stained with cTnT (green) and DAPI (blue) (n = 5, scale bar = 10 μm). *P < 0.05 compared with control, #P < 0.05 compared with PE group, $P < 0.05 compared with PE + CAP group.
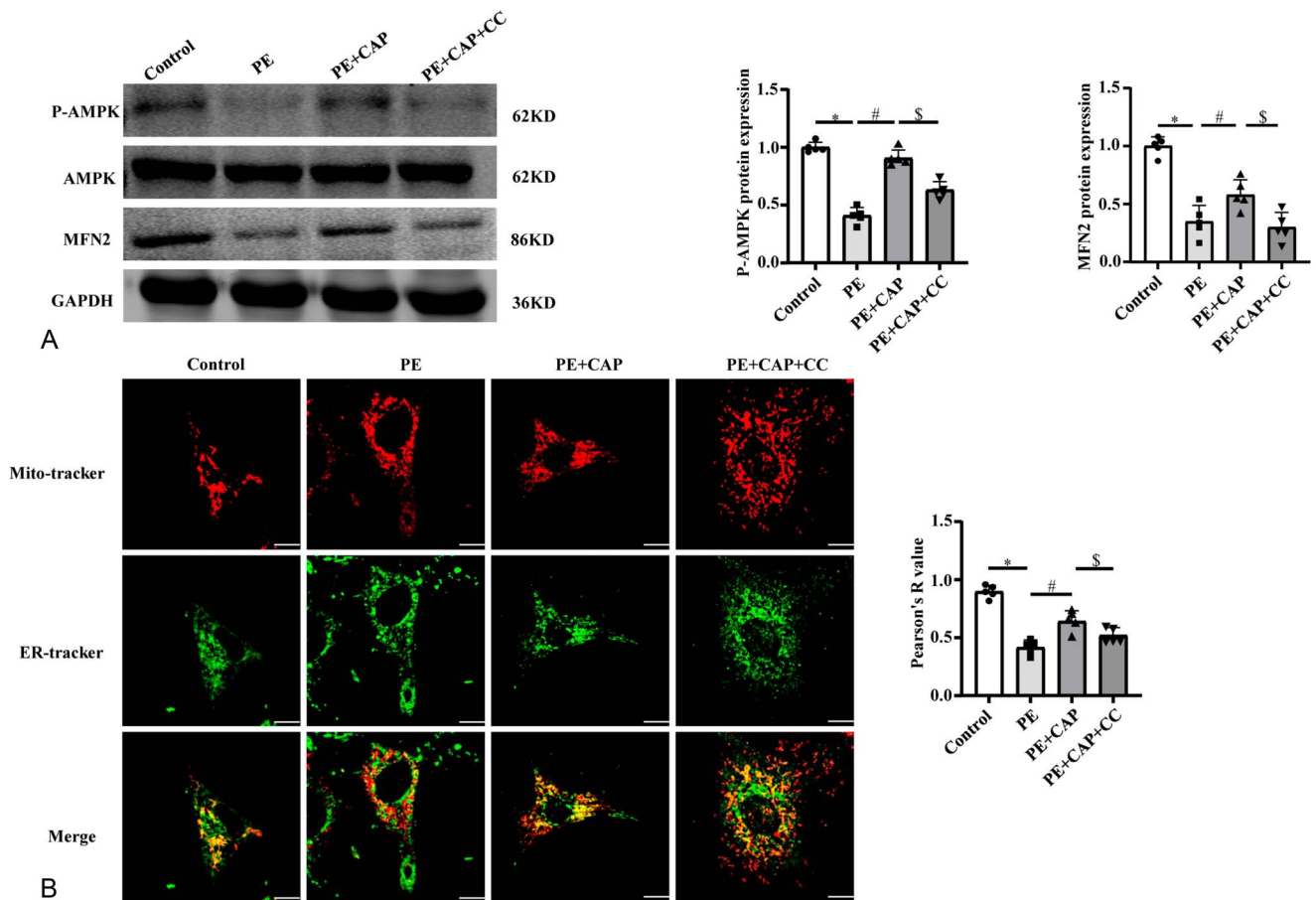
FIGURE 7. TRPV1 activation promotes MAM formation via AMPK/MFN2 pathway. A, The p-AMPK, AMPK, MFN2 protein expression in primary cardiomyocytes treated with capsaicin and CC (n = 5). B, Representative confocal images showing the association between ER (ER-Tracker Green) and mitochondria (MitoTracker Red) in cardiomyocytes (scale bar = 10 μm). Quantitation of ER-mitochondria contacts using the Pearson's coefficient (n = 5). *$P < 0.05$ compared with control, #$P < 0.05$ compared with PE group, $$P < 0.05$ compared with PE + CAP group.

works with MFN1 as a heterodimer to control mitochondrial outer membrane fusion.[48,49] Several studies have shown that the AMPK-MFN2 axis regulates MAM dynamics and mitochondrial fusion under energy stress or disease conditions.[28,50–52] Consistent with the reported literature, we discovered that siMFN2 could inhibit the protective effect of TRPV1 on the mitochondria, suggesting that TRPV1 activation protects mitochondria by promoting MAM formation via the AMPK/MFN2 pathway during myocardial hypertrophy. Although MFN2 is important for MAM formation, MAM is more than an organelle membrane fusion region where mitochondrial and ER membrane proteins mutually compete with each other to build a complicated subdomain.[53]

Membrane proteins and lipid membrane structures play important roles in MAM function. Previous studies focused on the functions of mitochondrial outer membrane proteins and ER proteins and found that a variety of proteins are involved in MAM formation. However, further studies reported that the knockout of different membrane proteins could only partially inhibit MAM formation.[54] Therefore, studies of the interaction between mitochondrial outer

membrane proteins and ER proteins alone could not fully elucidate the mechanism of MAM formation and functional regulation, whereas other factors may play a more important role in MAM formation, among which the structural conformation and composition changes of the mitochondrial outer membrane are important factors. Studies have confirmed that changes in the conformation and composition of the mitochondrial outer membrane can affect MMP, fluidity, and permeability, whereas changes in the expression and stability of membrane proteins will lead to disordered MAM formation and substance exchange.[55,56] Nevertheless, the effect of the TRPV1-AMPK/MFN2-MAM pathway on mitochondrial function and dynamics in myocardial hypertrophy requires further study.

In the present study, we verified that TRPV1 protects pressure overload-induced cardiac remodeling, indicating that capsaicin or other TRPV1 agonists may act as a prophylactic agent against mitochondrial injury in patients with myocardial hypertrophy diseases. However, some studies reported that TRPV1-AMPK pathway activation antagonizes diabetic nephropathy by inhibiting MAM contact in podocytes.[57]

We speculated that, first of all, different disease models may have different underlying mechanisms and effects, and physiological phenomena may vary immensely, or even reverse; second, TRPV1 can maintain the dynamic equilibrium of MAM to a certain extent. Under stress conditions, TRPV1 can promote MAM formation and relieve mitochondrial pressure; however, when excessive MAM leads to mitochondrial dysfunction, TRPV1 can inhibit MAM formation and protect mitochondrial homeostasis.

However, the distance between ER and mitochondria increases and MAM decreases in myocytes treated with norepinephrine, reducing mitochondrial Ca^{2+} reuptake.[58] In addition, studies have reported that reduction of MAM resulted in low Ca^{2+} exchange efficiency.[59–61] All of these studies suggest that the heart failure lacks the function of mitochondrial Ca^{2+} reuptake, which is because of the decrease of MAM. More importantly, these findings highlight the role of MAM involvement in mitochondrial calcium homeostasis in maintaining normal cardiac function. Therefore, we speculated that TRPV1 activates the AMPK-MFN2 axis and promotes MAM formation, protecting mitochondrial homeostasis in myocytes, would finally contribute to mitochondrial Ca^{2+} uptake, enhance the TCA (tricarboxylic acid) cycle (increased ATP production), and ultimately reverse cardiac hypertrophy. However, further studies are required to elucidate these hypotheses.

Numerous studies have found that TRPV1 plays an important role in hypertension, vascular calcification, diabetic nephropathy, and other diseases.[62–64] Thereby, TRPV1 is also considered an attractive target as agonists or antagonists for cardiovascular diseases.

Furthermore, the pharmaceutical industry has developed a number of different TRPV1 antagonists, several of which are undergoing clinical trials and none are currently in routine clinical use.[65] The main limitations of TRPV1 antagonists are accidental burns and hyperthermia side effects.[64] It is possible to develop antagonists that do not have these side effects. The increasing understanding of the regulation of TRPV1 channels and advances in the structural biology of TRPV1 channels provide the possibility for rational design of agonists and antagonists of TRPV1. We still expect TRPV1 can be used as a target in the research and development of new drugs for cardiac hypertrophy.

CONCLUSIONS

In conclusion, our data described the role of TRPV1 in alleviating myocardial hypertrophy damage via regulating MAM formation by affecting AMPK-MFN2 pathways, providing beneficial influence on mitochondrial homeostasis. Because TRPV1 is a key molecule in cardiovascular diseases, the domain and functional region of the protein may contribute to the development of new drugs for cardiovascular diseases.

REFERENCES

1. Nakamura M, Sadoshima J. Mechanisms of physiological and pathological cardiac hypertrophy. *Nat Rev Cardiol.* 2018;15:387–407.

2. Ritterhoff J, Young S, Villet O, et al. Metabolic remodeling promotes cardiac hypertrophy by directing glucose to aspartate biosynthesis. *Circ Res.* 2020;126:182–196.

3. Lips DJ, deWindt LJ, van Kraaij DJ, et al. Molecular determinants of myocardial hypertrophy and failure: alternative pathways for beneficial and maladaptive hypertrophy. *Eur Heart J.* 2003;24:883–896.

4. Yan Q, Tang J, Zhang X, et al. Does transient receptor potential vanilloid type 1 alleviate or aggravate pathological myocardial hypertrophy? *Front Pharmacol.* 2021;12:681286.

5. Zhong B, Rubinstein J, Ma S, et al. Genetic ablation of TRPV1 exacerbates pressure overload-induced cardiac hypertrophy. *Biomed Pharmacother.* 2018;99:261–270.

6. Wang Q, Ma S, Li D, et al. Dietary capsaicin ameliorates pressure overload-induced cardiac hypertrophy and fibrosis through the transient receptor potential vanilloid type 1. *Am J Hypertens.* 2014;27:1521–1529.

7. Gao F, Liang Y, Wang X, et al. TRPV1 activation attenuates high-salt diet-induced cardiac hypertrophy and fibrosis through PPAR-delta upregulation. *PPAR Res.* 2014;2014:491963.

8. Lang H, Li Q, Yu H, et al. Activation of TRPV1 attenuates high salt-induced cardiac hypertrophy through improvement of mitochondrial function. *Br J Pharmacol.* 2015;172:5548–5558.

9. Pfanner N, Warscheid B, Wiedemann N. Mitochondrial proteins: from biogenesis to functional networks. *Nat Rev Mol Cel Biol.* 2019;20:267–284.

10. Zhou Z, Torres M, Sha H, et al. Endoplasmic reticulum-associated degradation regulates mitochondrial dynamics in brown adipocytes. *Science.* 2020;368:54–60.

11. Luan Y, Luan Y, Yuan RX, et al. Structure and function of mitochondria-associated endoplasmic reticulum membranes (MAMs) and their role in cardiovascular diseases. *Oxid Med Cel Longev.* 2021;2021:4578809.

12. Wu S, Lu Q, Ding Y, et al. Hyperglycemia-driven inhibition of AMP-activated protein kinase alpha2 induces diabetic cardiomyopathy by promoting mitochondria-associated endoplasmic reticulum membranes in vivo. *Circulation.* 2019;139:1913–1936.

13. Dia M, Gomez L, Thibault H, et al. Reduced reticulum-mitochondria Ca(2+) transfer is an early and reversible trigger of mitochondrial dysfunctions in diabetic cardiomyopathy. *Basic Res Cardiol.* 2020;115:74.

14. de Brito OM, Scorrano L. Mitofusin 2 tethers endoplasmic reticulum to mitochondria. *Nature.* 2008;456:605–610.

15. Filadi R, Greotti E, Turacchio G, et al. On the role of Mitofusin 2 in endoplasmic reticulum-mitochondria tethering. *Proc Natl Acad Sci U S A.* 2017;114:E2266–E2267.

16. Hamasaki M, Furuta N, Matsuda A, et al. Autophagosomes form at ER-mitochondria contact sites. *Nature.* 2013;495:389–393.

17. Murley A, Lackner LL, Osman C, et al. ER-associated mitochondrial division links the distribution of mitochondria and mitochondrial DNA in yeast. *Elife.* 2013;2:e00422.

18. Zhao T, Huang X, Han L, et al. Central role of mitofusin 2 in autophagosome-lysosome fusion in cardiomyocytes. *J Biol Chem.* 2012;287:23615–23625.

19. Givvimani S, Pushpakumar S, Veeranki S, et al. Dysregulation of Mfn2 and Drp-1 proteins in heart failure. *Can J Physiol Pharmacol.* 2014;92:583–591.

20. Hu L, Ding M, Tang D, et al. Targeting mitochondrial dynamics by regulating Mfn2 for therapeutic intervention in diabetic cardiomyopathy. *Theranostics.* 2019;9:3687–3706.

21. Herzig S, Shaw RJ. AMPK: guardian of metabolism and mitochondrial homeostasis. *Nat Rev Mol Cel Biol.* 2018;19:121–135.

22. Toyama EQ, Herzig S, Courchet J, et al. Metabolism. AMP-activated protein kinase mediates mitochondrial fission in response to energy stress. *Science.* 2016;351:275–281.

23. Wu W, Li W, Chen H, et al. FUNDC1 is a novel mitochondrial-associated-membrane (MAM) protein required for hypoxia-induced mitochondrial fission and mitophagy. *Autophagy.* 2016;12:1675–1676.

24. Madhavi YV, Gaikwad N, Yerra VG, et al. Targeting AMPK in diabetes and diabetic complications: energy homeostasis, autophagy and mitochondrial Health. *Curr Med Chem.* 2019;26:5207–5229.

25. Garcia D, Hellberg K, Chaix A, et al. Genetic liver-specific AMPK activation protects against diet-induced obesity and NAFLD. *Cell Rep.* 2019;26:192–208.e6.

26. Wang Z, Wang N, Liu P, et al. AMPK and cancer. *Exp Suppl.* 2016;107:203–226.

27. Wu S, Zou MH. AMPK, mitochondrial function, and cardiovascular disease. *Int J Mol Sci.* 2020;21:21.
28. Hu Y, Chen H, Zhang L, et al. The AMPK-MFN2 axis regulates MAM dynamics and autophagy induced by energy stresses. *Autophagy.* 2021; 17:1142–1156.
29. Zaw AM, Williams CM, Law HK, et al. Minimally invasive transverse aortic constriction in mice. *J Vis Exp.* 2017;55293.
30. Jiang DS, Wei X, Zhang XF, et al. IRF8 suppresses pathological cardiac remodelling by inhibiting calcineurin signalling. *Nat Commun.* 2014;5: 3303.
31. Arruda AP, Pers BM, Parlakgül G, et al. Chronic enrichment of hepatic endoplasmic reticulum-mitochondria contact leads to mitochondrial dysfunction in obesity. *Nat Med.* 2014;20:1427–1435.
32. Barlow AL, Macleod A, Noppen S, et al. Colocalization analysis in fluorescence micrographs: verification of a more accurate calculation of pearson's correlation coefficient. *Microsc Microanal.* 2010;16:710–724.
33. Huang W, Mao L, Xie W, et al. Impact of UCP2 depletion on heat stroke-induced mitochondrial function in human umbilical vein endothelial cells. *Int J Hyperthermia.* 2022;39:287–296.
34. Juárez-Contreras R, Méndez-Reséndiz KA, Rosenbaum T, et al. TRPV1 channel: a noxious signal transducer that affects mitochondrial function. *Int J Mol Sci.* 2020;21.
35. Iftinca M, Defaye M, Altier C. TRPV1-Targeted drugs in development for human pain conditions. *Drugs.* 2021;81:7–27.
36. Bujak JK, Kosmala D, Szopa IM, et al. Inflammation, cancer and immunity-implication of TRPV1 channel. *Front Oncol.* 2019;9:1087.
37. Fisher JT. The TRPV1 ion channel: implications for respiratory sensation and dyspnea. *Respir Physiol Neurobiol.* 2009;167:45–52.
38. Peng J, Li YJ. The vanilloid receptor TRPV1: role in cardiovascular and gastrointestinal protection. *Eur J Pharmacol.* 2010;627:1–7.
39. Harb AA, Bustanji YK, Almasri IM, et al. Eugenol reduces LDL cholesterol and hepatic steatosis in hypercholesterolemic rats by modulating TRPV1 receptor. *Sci Rep.* 2019;9:14003.
40. Zhong B, Ma S, Wang DH. Knockout of TRPV1 exacerbates ischemia-reperfusion-induced renal inflammation and injury in obese mice. *In Vivo.* 2020;34:2259–2268.
41. Vemula P, Gautam B, Abela GS, et al. Myocardial ischemia/reperfusion injury: potential of TRPV1 agonists as cardioprotective agents. *Cardiovasc Hematol Disord Drug Targets.* 2014;14:71–78.
42. Hu R, Wang MQ, Ni SH, et al. Salidroside ameliorates endothelial inflammation and oxidative stress by regulating the AMPK/NF-κB/NLRP3 signaling pathway in AGEs-induced HUVECs. *Eur J Pharmacol.* 2020;867:172797.
43. Li Y, Chen Y. AMPK and autophagy. *Adv Exp Med Biol.* 2019;1206:85–108.
44. Chen YH, Yang SF, Yang CK, et al. Metformin induces apoptosis and inhibits migration by activating the AMPK/p53 axis and suppressing PI3K/AKT signaling in human cervical cancer cells. *Mol Med Rep.* 2021;23:88.
45. Yu LM, Dong X, Xue XD, et al. Naringenin improves mitochondrial function and reduces cardiac damage following ischemia-reperfusion injury: the role of the AMPK-SIRT3 signaling pathway. *Food Funct.* 2019;10:2752–2765.
46. Vance JE. MAM (mitochondria-associated membranes) in mammalian cells: lipids and beyond. *Biochim Biophys Acta.* 2014;1841:595–609.
47. Gao P, Yan Z, Zhu Z. Mitochondria-associated endoplasmic reticulum membranes in cardiovascular diseases. *Front Cel Dev Biol.* 2020;8: 604240.
48. Detmer SA, Chan DC. Complementation between mouse Mfn1 and Mfn2 protects mitochondrial fusion defects caused by CMT2A disease mutations. *J Cel Biol.* 2007;176:405–414.
49. Chen H, Detmer SA, Ewald AJ, et al. Mitofusins Mfn1 and Mfn2 coordinately regulate mitochondrial fusion and are essential for embryonic development. *J Cel Biol.* 2003;160:189–200.
50. Li P, Wang J, Zhao X, et al. PTEN inhibition attenuates endothelial cell apoptosis in coronary heart disease via modulating the AMPK-CREB-Mfn2-mitophagy signaling pathway. *J Cel Physiol.* 2020;235:4878–4889.
51. Yu H, Hong X, Liu L, et al. Cordycepin decreases ischemia/reperfusion injury in diabetic hearts via upregulating AMPK/Mfn2-dependent mitochondrial fusion. *Front Pharmacol.* 2021;12:754005.
52. Dong H, Zhou W, Xin J, et al. Salvinorin A moderates postischemic brain injury by preserving endothelial mitochondrial function via AMPK/Mfn2 activation. *Exp Neurol.* 2019;322:113045.
53. Janikiewicz J, Szymański J, Malinska D, et al. Mitochondria-associated membranes in aging and senescence: structure, function, and dynamics. *Cell Death Dis.* 2018;9:332.
54. Wu S, Zou MH. Mitochondria-associated endoplasmic reticulum membranes in the heart. *Arch Biochem Biophys.* 2019;662:201–212.
55. Lan B, He Y, Sun H, et al. The roles of mitochondria-associated membranes in mitochondrial quality control under endoplasmic reticulum stress. *Life Sci.* 2019;231:116587.
56. Mühleip A, McComas SE, Amunts A. Structure of a mitochondrial ATP synthase with bound native cardiolipin. *Elife.* 2019;8:8.
57. Wei X, Wei X, Lu Z, et al. Activation of TRPV1 channel antagonizes diabetic nephropathy through inhibiting endoplasmic reticulum-mitochondria contact in podocytes. *Metabolism.* 2020;105:154182.
58. Gutierrez T, Parra V, Troncoso R, et al. Alteration in mitochondrial Ca(2+) uptake disrupts insulin signaling in hypertrophic cardiomyocytes. *Cell Commun Signal.* 2014;12:68.
59. Wu S, Lu Q, Wang Q, et al. Binding of FUN14 domain containing 1 with inositol 1,4,5-trisphosphate receptor in mitochondria-associated endoplasmic reticulum membranes maintains mitochondrial dynamics and function in hearts in vivo. *Circulation.* 2017;136:2248–2266.
60. Bertero E, Maack C. Metabolic remodelling in heart failure. *Nat Rev Cardiol.* 2018;15:457–470.
61. Fernandez-Sanz C, Ruiz-Meana M, Miro-Casas E, et al. Defective sarcoplasmic reticulum-mitochondria calcium exchange in aged mouse myocardium. *Cel Death Dis.* 2014;5.
62. Yang D, Luo Z, Ma S, et al. Activation of TRPV1 by dietary capsaicin improves endothelium-dependent vasorelaxation and prevents hypertension. *Cell Metab.* 2010;12:130–141.
63. Luo DA-O, Li W, Xie C, et al. Capsaicin attenuates arterial calcification through promoting SIRT6-mediated deacetylation and degradation of Hif1α (Hypoxic-Inducible factor-1 alpha). *Hypertension.* 2022;79:906–917.
64. Nilius B, Szallasi A. Transient receptor potential channels as drug targets: from the science of basic research to the art of medicine. *Pharmacol Rev.* 2014;66:676–814.
65. Moran MM, McAlexander MA, Bíró T, et al. Transient receptor potential channels as therapeutic targets. *Nat Rev Drug Discov.* 2011;10:601–620.